PLAXIS

essential for geotechnical professionals

PLAXIS

Circular Tunnel Driven in Elastic Cross Anisotropic Rocks

2016

by

T.D.Y.F. Simanjuntak
Plaxis bv, The Netherlands

1. Introduction

Tunnels may be constructed in an inherently anisotropic rock mass, such as metamorphic rock. This type of rock, which is composed of lamination of intact rock, can take the form of cross anisotropy or transverse isotropy commonly configured by one direction of stratification planes perpendicular to the direction of deposition. Since such a rock formation can exhibit significant strength and deformability in the direction parallel and perpendicular to the stratification planes, the response of the rock mass to excavation can be different from that under the assumption of isotropic rocks.

2. Objectives

The study objective is to investigate the mechanical response of an elastic cross anisotropic or transversely isotropic rock mass to circular excavation subjected to either uniform or non-uniform in-situ stresses.

3. Hoop Stress and Radial Deformation

As long as the plane of cross anisotropy of the rock mass strikes parallel to the tunnel axis, the plane strain conditions are acceptable. Accordingly, the full mathematical treatise to calculate the excavation-induced hoop stresses and deformations along the perimeter of a circular tunnel embedded in such a rock mass with horizontal stratification planes is available in Hefny and Lo (1999). For completeness, they can be rewritten as follows (Simanjuntak, 2015):

Hoop Stress:

$$\sigma_o = \frac{2 + 2(\gamma_1 + \gamma_2)^2 - 2\gamma_1^2\gamma_2^2 - 4(\gamma_1 + \gamma_2)\cos 2\theta}{(1 + \gamma_1^2 - 2\gamma_1 \cos 2\theta)(1 + \gamma_2^2 - 2\gamma_2 \cos 2\theta)} \left(\frac{(k+1)\sigma_v}{2}\right) + \\ + \frac{4(\gamma_1 + \gamma_2) - 4(1 + \gamma_1\gamma_2)\cos 2\theta}{(1 + \gamma_1^2 - 2\gamma_1 \cos 2\theta)(1 + \gamma_2^2 - 2\gamma_2 \cos 2\theta)} \left(\frac{(k-1)\sigma_v}{2}\right) \quad (1)$$

with

$$\gamma_1 = \frac{\mu_1 - 1}{\mu_1 + 1}; \quad |\gamma_1| < 1$$
$$\gamma_2 = \frac{\mu_2 - 1}{\mu_2 + 1}; \quad |\gamma_2| < 1 \quad (2)$$
$$\mu_1^2 \mu_2^2 = \frac{S_{11}}{S_{22}}$$
$$\mu_1^2 + \mu_2^2 = \frac{2S_{12} + S_{33}}{S_{22}}$$

where:

$$
\begin{aligned}
S_{11} &= \frac{1 - \nu_h^2}{E_h} \\
S_{22} &= \frac{1 - \nu_{hv}\ \nu_{vh}}{E_v} \\
S_{12} &= S_{21} = -\frac{\nu_{vh}\ (1 + \nu_h)}{E_v} \\
S_{33} &= \frac{1}{G_{vh}}
\end{aligned}
\tag{3}
$$

in which E_h and E_v are the Young's modulus in the plane of isotropy and in the direction normal to the plane of isotropy respectively, ν_h is the Poisson's ratio in the plane of isotropy, ν_{hv} is the Poisson's ratio for the effect of stress in the plane of isotropy on the strain in the direction normal to the plane of isotropy, ν_{vh} is the Poisson's ratio for the effect of stress normal to the plane of isotropy on the strain in the plane of isotropy, and G_{vh} is the shear modulus normal to the plane of isotropy.

The in-situ horizontal stress in the rock mass, σ_h, can be expressed as the product of the in-situ vertical stress, σ_v, and a coefficient of earth pressure, k. The mean in-situ stress, σ_o, can be defined as (Carranza-Torres and Fairhurst, 2000):

$$
\sigma_o = \frac{\sigma_v + \sigma_h}{2} = \frac{(k+1)\ \sigma_v}{2} \tag{4}
$$

in which: $k < 1$ if the in-situ vertical stress is greater than the in-situ horizontal stress, and
$k > 1$ if the in-situ horizontal stress is greater than the in-situ vertical stress.

Radial Deformation:

$$
\begin{aligned}
u_r = {} & \frac{R}{2\ (\gamma_1 - \gamma_2)} \cdot \\
& \cdot \left\{ \left(\frac{(k+1)\ \sigma_v}{2} \right) (\gamma_2\ \rho_1 - \gamma_1\ \rho_2) + \left(\frac{(k-1)\ \sigma_v}{2} \right) (\rho_1 - \rho_2) + \right. \\
& \left. + \left[\left(\frac{(k+1)\ \sigma_v}{2} \right) (\gamma_2\ \delta_1 - \gamma_1\ \delta_2) + \left(\frac{(k-1)\ \sigma_v}{2} \right) (\delta_1 - \delta_2) \right] \cos 2\theta \right\}
\end{aligned}
\tag{5}
$$

with

$$
\begin{aligned}
\delta_1 &= (1 + \gamma_1)\ \beta_2 - (1 - \gamma_1)\ \beta_1 \\
\delta_2 &= (1 + \gamma_2)\ \beta_1 - (1 - \gamma_2)\ \beta_2 \\
\rho_1 &= (1 + \gamma_1)\ \beta_2 + (1 - \gamma_1)\ \beta_1 \\
\rho_2 &= (1 + \gamma_2)\ \beta_1 + (1 - \gamma_1)\ \beta_2
\end{aligned}
\tag{6}
$$

and

$$
\begin{aligned}
\beta_1 &= S_{12} - S_{22}\ \mu_1^2 \\
\beta_2 &= S_{12} - S_{22}\ \mu_2^2
\end{aligned}
\tag{7}
$$

4. Numerical Results

As an example, a circular tunnel with a radius, R, of 2 m is excavated though an elastic cross anisotropic or transversely isotropic rock mass subjected to the mean in-situ stresses, σ_o, of 40 MPa. Herein, the dipping angle, α, is zero meaning that the stratification planes are horizontal. There are three cases studied by varying the in-situ stress ratio coefficient. Case A is for k equals 1.00, Case B for k equals 0.80, and Case C for k equals 1.25.

When modelling anisotropy, distinction can be made between the elastic anisotropy and the plastic anisotropy. Elastic anisotropy refers to the use of different elastic stiffness properties in different directions, which can be described by five elastic parameters, while plastic anisotropy may involve the use of different strength properties in different directions.

In this study, the elasto-plastic Jointed Rock model was used. The elastic response of the cross anisotropic rocks to circular excavation was ensured by providing an adequate cohesion along the sliding planes (Wittke, 1990; Tonon and Amadei, 2003; Tonon, 2004; Simanjuntak et al. 2014). The five independent rock parameters required to simulate the stress-strain behaviour in the elastic range are given in Table 1.

Table 1. Rock Data (Hefny and Lo, 1999)

E_h (GPa)	E_v (GPa)	G_{vh} (GPa)	ν_{vh}	ν_h
15.8	10.5	3.95	0.30	0.30

For cases when the in-situ stresses in the rock mass are uniform or k is equal to 1.00, the distribution of radial deformations in the space around the tunnel as a result of excavation is shown in Fig. 1a. The predicted maximum radial deformation is 10.36 mm and is located at the tunnel roof and invert, while the minimum radial deformation is 8.23 mm and is found at the tunnel sidewalls. This implies that the tunnel is oval with its major axis parallel to the direction of stratification planes.

For cases when the in-situ stress ratio, k, is equal to 0.80 representing the in-situ vertical stress greater than the horizontal, the predicted distribution of radial deformations around the tunnel is illustrated in Fig. 2a. It is seen that as great as 12.08 mm of deformation in radial direction was found at the tunnel roof and invert, whereas at the tunnel sidewalls it was 6.75 mm. This indicates that the tunnel remains oval with its major axis parallel to the direction of stratification planes and since the in-situ vertical stress is greater than the horizontal, this also contributes to a greater deformation at the tunnel roof and invert.

When the in-situ stress ratio, k, is equal to 1.25 representing the in-situ horizontal stress greater than the vertical, the predicted distribution of radial deformations is depicted in Fig. 3a. Here, the predicted maximum deformation is 9.73 mm and is located at the tunnel sidewalls, while the minimum deformation is 8.63 mm and is situated at the tunnel roof and invert. This suggests that the tunnel is oval; however, its major axis is perpendicular to the direction of stratification planes.

In view of model validation, the numerical result of radial deformations are compared with those calculated using the analytical solution. The predicted and calculated radial deformations along the tunnel perimeter, θ, are depicted in Fig. 4. It is seen that the numerical results using PLAXIS are in good agreement with those calculated using the analytical solution, rendering that the numerical approach presented herein are methodologically correct. The predicted and calculated results of radial deformations are summarised in Table 2.

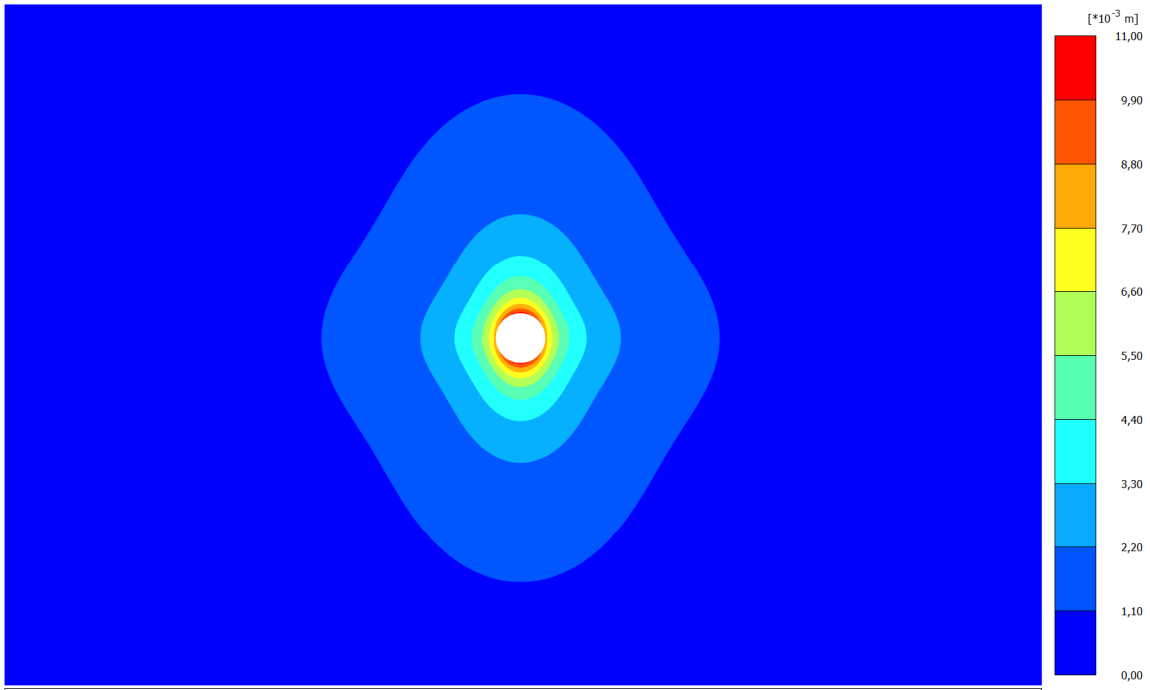

Total displacements |u|

Maximum value = 0,01036 m (Element 509 at Node 6741)

(a)

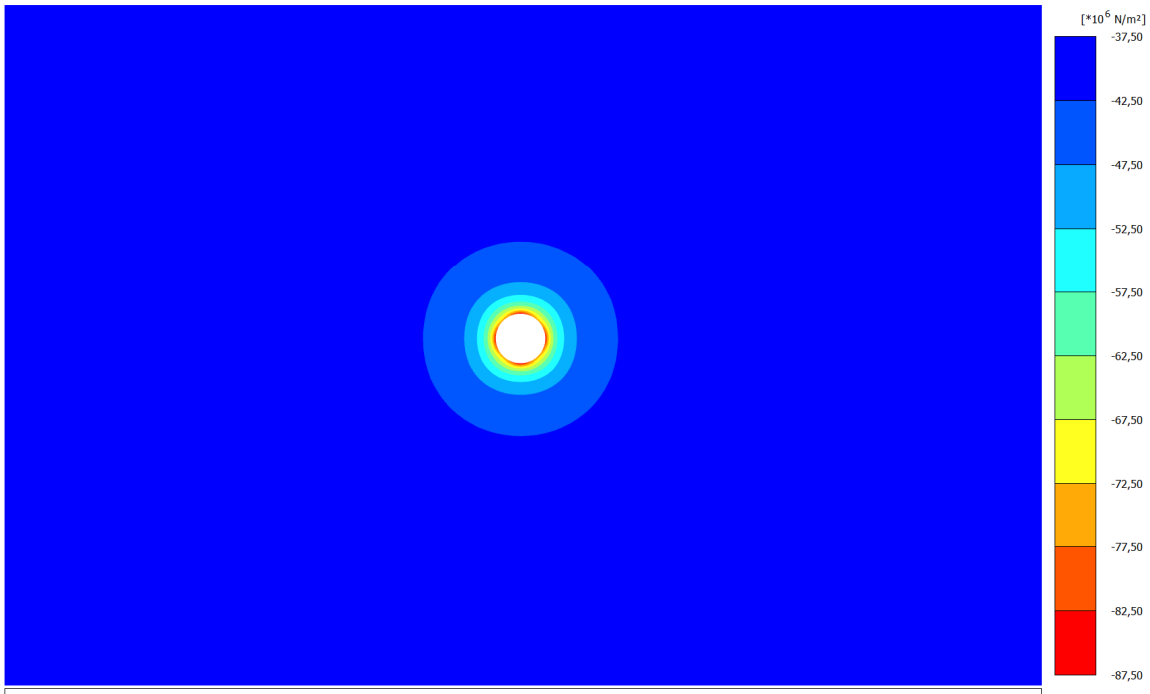

Principal total stress σ_1

Maximum value = -39,95*10^6 N/m² (Element 637 at Node 1613)

Minimum value = -85,20*10^6 N/m² (Element 538 at Node 3096)

(b)

Fig. 1. Case A (k = 1.00) - Distribution of (a) Radial Deformations and (b) Hoop Stresses

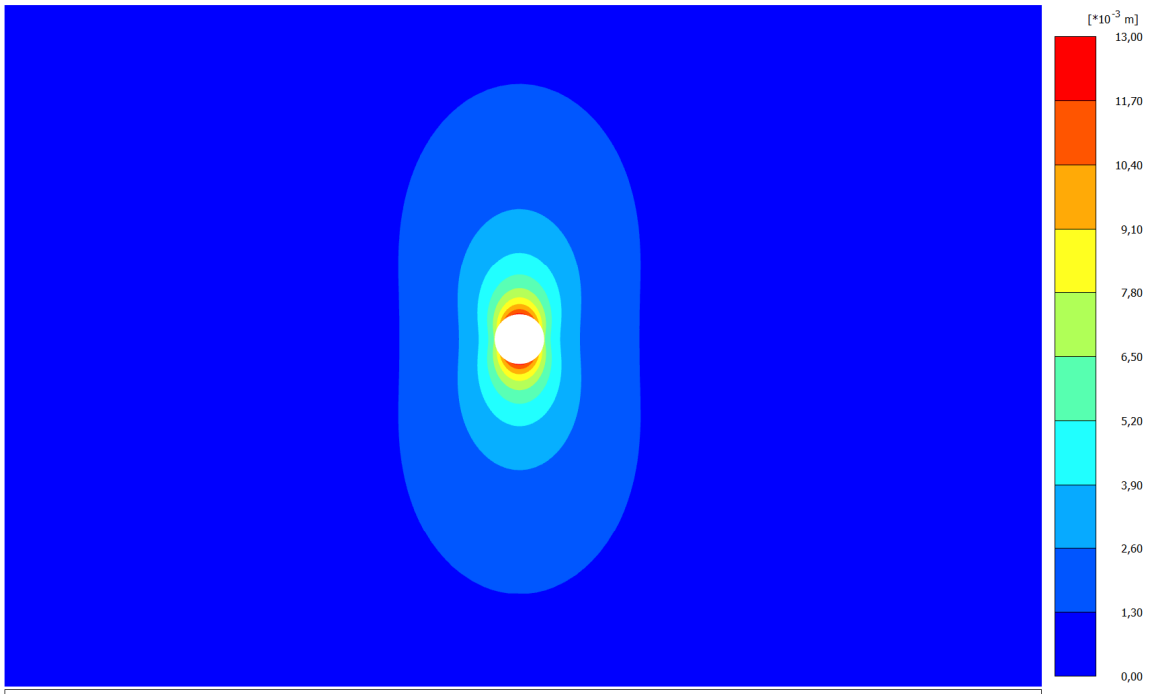

Total displacements |u|

Maximum value = 0,01208 m (Element 509 at Node 6741)

(a)

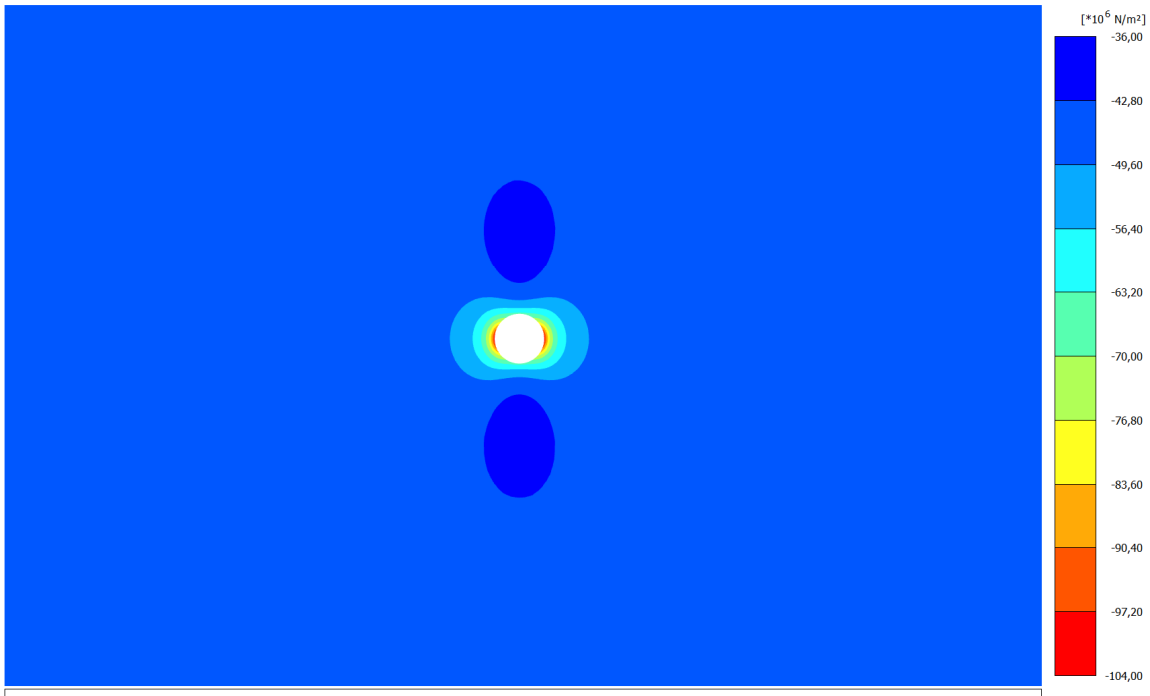

Principal total stress σ_1

Maximum value = -39,04*10^6 N/m² (Element 2256 at Node 5424)

Minimum value = -101,2*10^6 N/m² (Element 551 at Node 3571)

(b)

Fig. 2. Case B (k = 0.80) - Distribution of (a) Radial Deformations and (b) Hoop Stresses

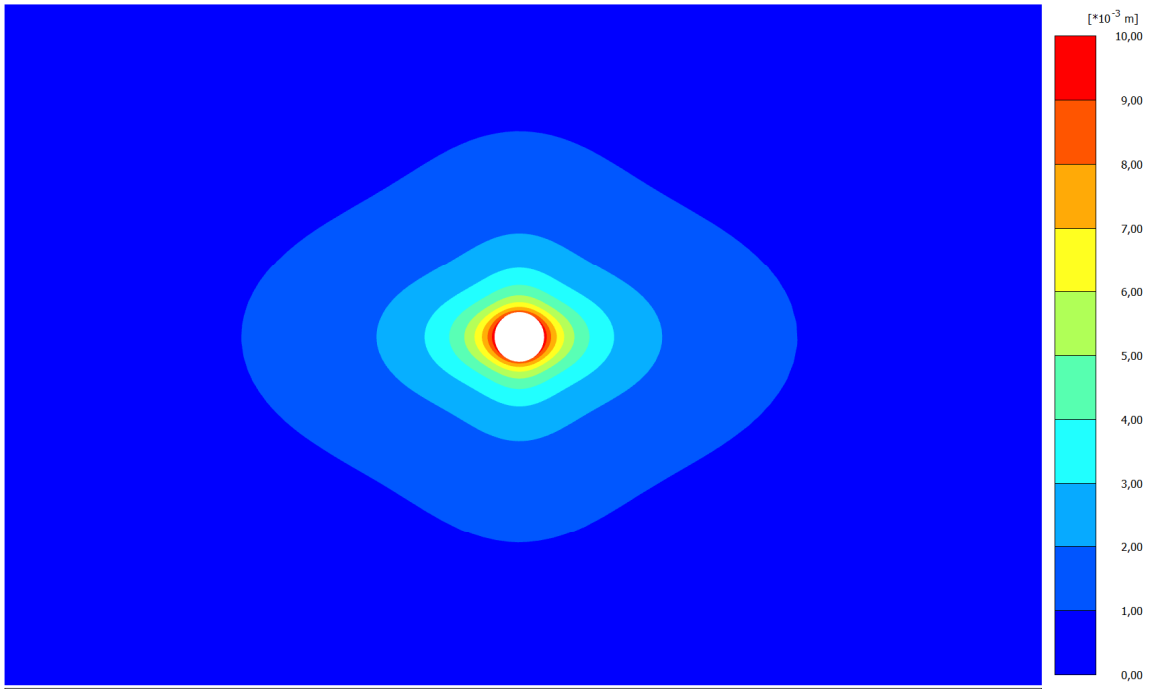

Total displacements |u|

Maximum value = 9,729*10^{-3} m (Element 537 at Node 4872)

(a)

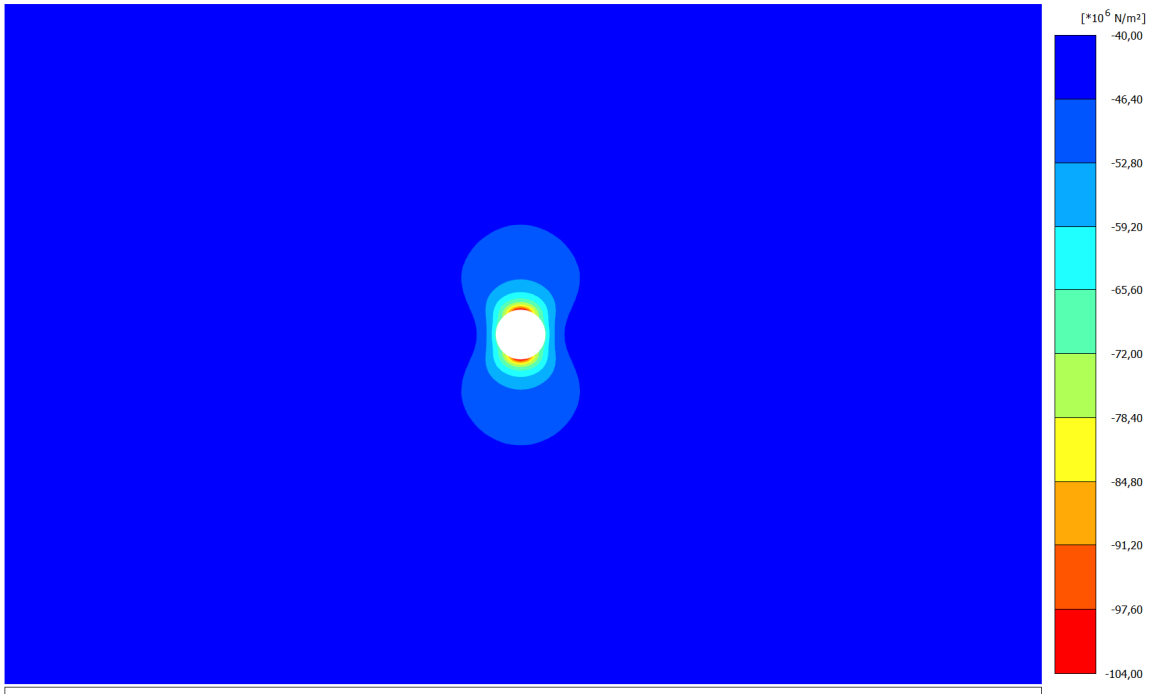

Principal total stress σ_1

Maximum value = -43,76*10^{6} N/m² (Element 222 at Node 8639)

Minimum value = -103,8*10^{6} N/m² (Element 503 at Node 3251)

(b)

Fig. 3. Case C (k = 1.25) - Distribution of (a) Radial Deformations and (b) Hoop Stresses

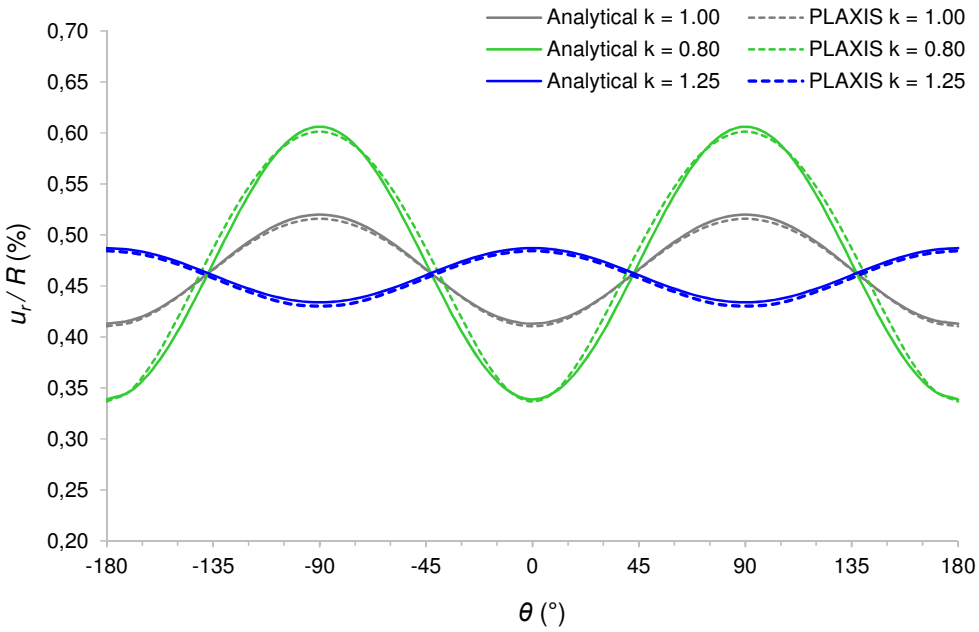

Fig. 4. Comparison of Radial Deformations between Analytical Solution and PLAXIS

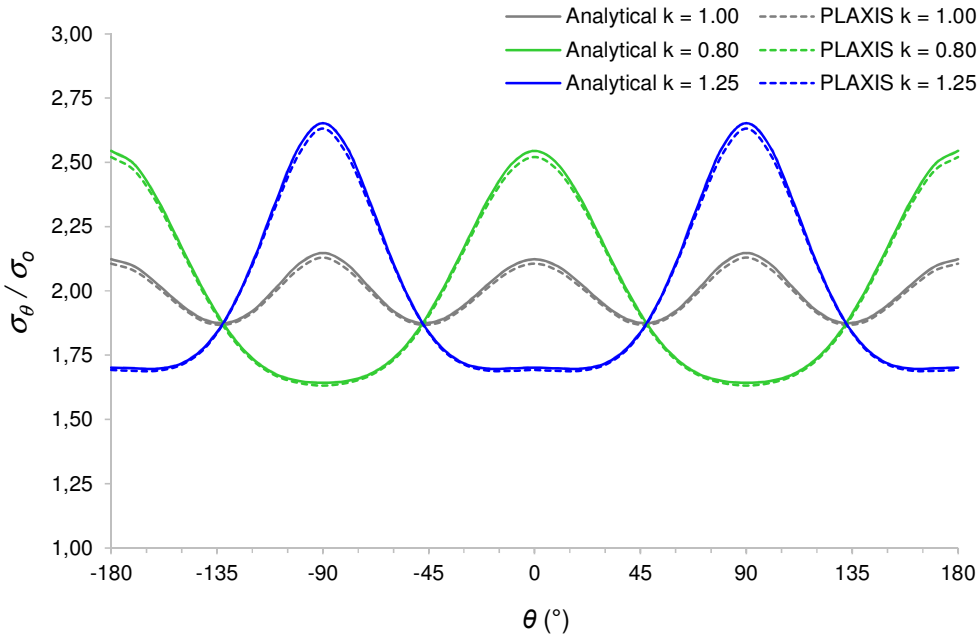

Fig. 5. Comparison of Hoop Stresses between Analytical Solution and PLAXIS

Analogously, the predicted distribution of hoop stresses in the rock mass as a result of tunnel excavation for cases when the in-situ stresses in the rock mass are uniform or k is equal to 1.00, is shown in Fig. 1b. The maximum hoop stress of 85.20 MPa in compressive state of stress is found at the tunnel roof and invert. For the case when the in-situ stress ratio, k, is 0.80, as high as 101.23 MPa of hoop stresses is situated at the tunnel sidewalls (Fig. 2b). If the in-situ stress ratio, k, is 1.25, the maximum hoop stress is found as 103.82 MPa and is located at the tunnel roof and invert (Fig. 3b). The comparison of the distribution of hoop stresses along the tunnel perimeter, θ, obtained using PLAXIS and the analytical solution is presented in Fig. 5. It is seen that the numerical results fit the results calculated using the analytical solution with great accuracy. The predicted and calculated hoop stresses along the tunnel perimeter are given in Table 3.

Table 2. Predicted and Calculated Radial Displacements along the Tunnel Perimeter

θ (°)	u_r/R (%)					
	k = 1.00		k = 0.80		k = 1.25	
	Analytical	PLAXIS	Analytical	PLAXIS	Analytical	PLAXIS
0	0,413	0,410	0,339	0,337	0,487	0,484
10	0,416	0,414	0,347	0,347	0,486	0,483
20	0,425	0,424	0,370	0,377	0,481	0,478
30	0,440	0,439	0,406	0,419	0,474	0,471
40	0,457	0,457	0,449	0,464	0,465	0,462
50	0,476	0,475	0,496	0,508	0,456	0,453
60	0,493	0,491	0,539	0,547	0,447	0,444
70	0,507	0,504	0,575	0,576	0,440	0,437
80	0,517	0,513	0,598	0,595	0,435	0,432
90	0,520	0,516	0,606	0,601	0,434	0,430
100	0,517	0,513	0,598	0,595	0,435	0,432
110	0,507	0,504	0,575	0,576	0,440	0,437
120	0,493	0,491	0,539	0,547	0,447	0,444
130	0,476	0,475	0,496	0,508	0,456	0,453
140	0,457	0,457	0,449	0,464	0,465	0,462
150	0,440	0,439	0,406	0,419	0,474	0,471
160	0,425	0,424	0,370	0,377	0,481	0,478
170	0,416	0,414	0,347	0,347	0,486	0,483
180	0,413	0,410	0,339	0,337	0,487	0,484
190	0,416	0,414	0,347	0,347	0,486	0,483
200	0,425	0,424	0,370	0,377	0,481	0,478
210	0,440	0,439	0,406	0,419	0,474	0,471
220	0,457	0,457	0,449	0,464	0,465	0,462
230	0,476	0,475	0,496	0,508	0,456	0,453
240	0,493	0,491	0,539	0,547	0,447	0,444
250	0,507	0,504	0,575	0,576	0,440	0,437
260	0,517	0,513	0,598	0,595	0,435	0,432
270	0,520	0,516	0,606	0,601	0,434	0,430
280	0,517	0,513	0,598	0,595	0,435	0,432
290	0,507	0,504	0,575	0,576	0,440	0,437
300	0,493	0,491	0,539	0,547	0,447	0,444
310	0,476	0,475	0,496	0,508	0,456	0,453
320	0,457	0,457	0,449	0,464	0,465	0,462
330	0,440	0,439	0,406	0,419	0,474	0,471
340	0,425	0,424	0,370	0,377	0,481	0,478
350	0,416	0,414	0,347	0,347	0,486	0,483
360	0,413	0,410	0,339	0,337	0,487	0,484

Table 3. Predicted and Calculated Hoop Stresses along the Tunnel Perimeter

θ (°)	σ_θ / σ_o					
	k = 1.00		k = 0.80		k = 1.25	
	Analytical	PLAXIS	Analytical	PLAXIS	Analytical	PLAXIS
0	2,123	2,106	2,545	2,521	1,702	1,692
10	2,095	2,078	2,491	2,467	1,699	1,688
20	2,024	2,012	2,351	2,334	1,697	1,690
30	1,944	1,935	2,169	2,158	1,718	1,713
40	1,887	1,879	1,990	1,980	1,784	1,778
50	1,877	1,870	1,842	1,833	1,911	1,908
60	1,922	1,915	1,738	1,731	2,106	2,099
70	2,011	1,999	1,676	1,670	2,346	2,329
80	2,106	2,087	1,649	1,642	2,562	2,534
90	2,148	2,130	1,643	1,632	2,652	2,631
100	2,106	2,087	1,649	1,642	2,562	2,534
110	2,011	1,999	1,676	1,670	2,346	2,329
120	1,922	1,915	1,738	1,731	2,106	2,099
130	1,877	1,870	1,842	1,833	1,911	1,908
140	1,887	1,879	1,990	1,980	1,784	1,778
150	1,944	1,936	2,169	2,158	1,718	1,713
160	2,024	2,012	2,351	2,335	1,697	1,690
170	2,095	2,079	2,491	2,468	1,699	1,689
180	2,123	2,106	2,545	2,521	1,702	1,692
190	2,095	2,078	2,491	2,467	1,699	1,688
200	2,024	2,012	2,351	2,334	1,697	1,690
210	1,944	1,935	2,169	2,158	1,718	1,713
220	1,887	1,879	1,990	1,980	1,784	1,778
230	1,877	1,870	1,842	1,833	1,911	1,908
240	1,922	1,915	1,738	1,731	2,106	2,099
250	2,011	1,999	1,676	1,670	2,346	2,329
260	2,106	2,087	1,649	1,642	2,562	2,534
270	2,148	2,130	1,643	1,632	2,652	2,631
280	2,106	2,087	1,649	1,642	2,562	2,534
290	2,011	1,999	1,676	1,670	2,346	2,329
300	1,922	1,915	1,738	1,731	2,106	2,099
310	1,877	1,870	1,842	1,833	1,911	1,908
320	1,887	1,879	1,990	1,980	1,784	1,778
330	1,944	1,936	2,169	2,158	1,718	1,713
340	2,024	2,012	2,351	2,335	1,697	1,690
350	2,095	2,079	2,491	2,468	1,699	1,689
360	2,123	2,106	2,545	2,521	1,702	1,692

5. Concluding Remarks

This report presents the mechanical response of an elastic cross anisotropic or transversely isotropic rock mass to circular excavation subjected to uniform and non-uniform in-situ stresses. It was assumed that the plane of cross anisotropy (transverse isotropy) strikes parallel to the tunnel axis so that the plane strain conditions are applicable. Accordingly, a two-dimensional model is adequate to investigate the deformations and stresses around the excavation.

The anisotropic rock mass being considered has horizontal planes and in one direction. With regard to the in-situ stresses in the rock mass, there are three cases studied herein. In the first case, the in-situ stresses are uniform or the in-situ stress ratio is equal to 1.00. In the second case, the in-situ vertical stress is greater than the horizontal with a ratio, *k*, of 0.80. In the third case, the in-situ horizontal stress is greater than the vertical with a ratio, *k*, of 1.25.

In view of model validation, the numerical results obtained using PLAXIS are compared with the results calculated using the analytical solution. This study suggests that there is a global coherence between the numerical and analytical results, implying that the numerical approach is methodologically correct and can be applied for other cases within the scope of the study.

6. References

Carranza-Torres, C., Fairhurst, C. (2000). Application of the Convergence-Confinement Method of Tunnel Design to Rock Masses that Satisfy the Hoek-Brown Failure Criterion. *Tunnelling and Underground Space Technology*, 15(2), pp. 187–213.

Hefny, A.M., Lo, K.Y. (1999). Analytical Solutions for Stresses and Displacements Around Tunnels Driven in Cross-Anisotropic Rocks. *International Journal for Numerical and Analytical Methods in Geomechanics*, 23(2), pp. 161–177.

Simanjuntak, T.D.Y.F., Marence, M., Mynett, A.E., Schleiss, A.J. (2014). Effect of Rock Mass Anisotropy on Deformations and Stresses around Tunnels During Excavation. *The 82nd Annual Meeting of ICOLD*, *In Proceedings of the International Symposium on Dams in Global Environmental Challenges, Bali, Indonesia. pp. II-129 – II-136*.

Simanjuntak, T.D.Y.F. (2015). *Prestressed Concrete-lined Pressure Tunnels - Towards Improved Safety and Economincal Design*, PhD Thesis, Crc Press.

Tonon, F. (2004). Does Elastic Anisotropy Significantly Affect a Tunnel's Plane Strain Behavior? *Transportation Research Record: Journal of the Transportation Research Board*, (1868), pp. 156–168.

Tonon, F., Amadei, B. (2003). Stresses in Anisotropic Rock Masses: An Engineering Perspective Building on Geological Knowledge. *International Journal of Rock Mechanics and Mining Sciences*, 40(7), pp. 1099–1120.

Wittke, W. (1990). Rock Mechanics: Theory and Applications, with Case Histories. Springer Berlin.